FRACTURE ENERGY OF STEEL FIBRE REINFORCED CONCRETE

J.A.O. Barros[(1)], J. Sena Cruz[(2)]
Dep. of Civil Eng. – School of Eng. – University of Minho
Campus de Azurém, 4810 Guimarães CODEX
(1) barros@eng.uminho.pt,
(2) jsena@eng.uminho.pt

Abstract: Steel fibre reinforced concrete (*SFRC*) is a cementitious material reinforced with a given content of discrete fibres. The use of *SFRC* in building construction has increased continuously due to its better mechanical properties, mainly, the energy absorption capacity. The energy dissipated to pull out the fibres from the cracked concrete is much higher than the energy dissipated to crack the concrete matrix. Therefore, the energy absorption capacity is the main material property benefited by fibre reinforcement. A servo-controlled equipment should be used to evaluate this property. The tests should be carried out using displacement control in order to obtain the post-peak force-displacement relationship (tensile strain-softening branch).

In the present work it is described the three point bending notched *SFRC* beam tests carried out using displacement control. Series of beams reinforced with 30, 60 and 90 kg/m^3 of hooked ends steel fibres were tested. The main purpose of these tests was the evaluation of the fracture energy of SFRC. However, the energy evaluated from the force-displacement relationship registered in a test can be not only the energy dissipated in fracturing the concrete, but also the energy absorbed in compression deformation. For ductile materials like concrete reinforced with high content of fibres, the "fixed" points of the "Japenese Yok" bar may not remain fixed, which introduces extraneous deformations, leading to incorrect evaluation of the fracture energy. These factors were analysed in the present work in order to assess the appetence of the specimen dimensions and test procedures for evaluating the fracture energy of SFRC.

Keywords: Steel fibre reinforced concrete, fracture energy, strain softening, toughness

1 – INTRODUCTION

In the last two decades it has been done efforts in order to achieve a total or a partial substitute of conventional reinforcement on concrete. In this way, several discrete fibres were developed for concrete reinforcement, namely, steel, glass, synthetic and natural fibres[1,2]. Steel fibres are the most used in concrete applications due to the following main reasons: economy, manufacture facilities, reinforcing effects and resistance to the environment aggressiveness. The industrial floors, the tunnelling lines and the prefabrication are the main applications of steel fibre reinforced concrete (SFRC), where the conventional reinforcement is replaced by a given fibre content[3-7].

The energy absorption capacity of plain concrete is reduced. The ability of SFRC to absorb energy has been long recognized[1,8,9] as one of the most important benefits of the incorporation of fibres in plain concrete. For content of fibres used in practice, the increase on compression, tensile, shear and torsional strength is only marginal[1]. In structures with super abundant supports, like slabs on soil and tunnelling lines, the increase on the material energy absorption capacity provided by fibre reinforcement enhances the cracking behaviour and increases the load bearing capacity of these structures[5,6]. Due to the relevance of the energy absorption capacity on fibrous concrete, several procedures have been proposed to evaluate this property[8,10], resulting in some entities that are intended to reproduce this property, namely, the toughness indexes, the equivalent flexural strength and the fracture energy. Among these entities, the fracture energy is the most accepted and used on numerical models[7,11,14] . The other entities have reduced application on numerical simulation of SFRC structures[15].

The accuracy of a numerical simulation of a nonlinear behaviour of concrete structures depends significantly on the material fracture energy, G_f, which is defined as the amount of energy necessary to create one unit area of a crack[16]. The fracture energy can be evaluated from uniaxial tensile tests or bending tests using displacement control. The uniaxial tensile test is the most appropriate, but the test stability requires very stiff equipment[17,18]. Since this equipment is not available for the major part of the laboratories, three- or four-point bending tests on notched beams were usually carried out to evaluate the material fracture energy. The three-point bending tests on centre-notched beams are lesser used but are, perhaps, more suitable to characterise the fracture parameters of SFRC[19].

The present work aims to contribute to the knowledge about the fracture energy of SFRC. For this purpose, three-point bending tests on SFRC notched beams were carried out. Based on the data registered in the tests, the stress in notched cross section, the energy dissipated and the fracture energy were evaluated. The specimen dimensions and the test procedures proposed by RILEM[16] for evaluating the fracture energy of plain concrete could be not appropriate for fibrous concrete. Due to the higher deformability of SFRC over plain concrete, the energy dissipated in compression and the extraneous displacements on the "fixed" points of the bar supporting the displacement transducer could be not marginal. The significance of these phenomenons on the evaluation of the fracture energy is discussed in the present work.

2 – MATERIALS AND SPECIMENS

2.1 - Fibres

In this work it was used steel fibres with the trademark[20] Dramix ZP30/.50. These fibres have 30 mm length and 0.5 mm diameter, with a fibre aspect ratio of $l_f / d_f = 30 / 0.5 = 60$. They are glued together side by side into bundles of about 30 fibres with a water solvable glue in order to perform better in fresh concrete, improving the mix workability and eliminating balling[1]. The main characteristics of the fibres are presented in Table 1.

Table 1 – Main characteristics of *Dramix* ZP30/.50 hooked ends steel fibres.

Fibre type	Density (g/cm^3)	Tensile strength (MPa)	Elasticity modulus (GPa)	Ultimate strain (%)
ZP30/.50	7.8	1250	200	3 a 4

2.2 - Concrete

The mix composition used is described in table 2. More details about the mix composition and mixing procedures can be found elsewhere[21].

Table 2 – Concrete composition.

Element	Composition (kg/m^3 of concrete)
Cement	450
Sand (0-3 mm)	729
Coarse aggregate (0-15mm)	1000
Water	202.5
Fibres	0, 30, 60, 90

The uniaxial compression strength, f_{cm}, the tangent moduli, E_{ci}, and reduced moduli, E_{c1}, of elasticity[22] are included in table 3. These results are the average values of, at least, 5 cylinder specimens of 150 mm diameter and 300 mm height. The tests were carried out using displacement control. The manufacture of the specimens, the equipment and the test procedures were described in another work[21].

Table 3 – Compression strength and moduli of elasticity.

Property	0 kg/m^3	30 kg/m^3	60 kg/m^3	90 kg/m^3
f_{cm} (MPa)	36.1	33.9	34.4	33.5
E_{ci} (GPa)	31.9	25.1	26.0	27.2
E_{c1} (GPa)	20.9	16.6	15.4	15.0

2.3 – Bending notched beam specimens

The specimens were compacted on a vibrating table in order to assure a dense mix and an uniform distribution of fibres. The specimens for bending tests have the dimensions recommended by RILEM for evaluating the material fracture energy on plain concrete[16]: 800×100×100 mm^3. Since the ratio between the compressive and the tensile strength of the SFRC tested in this work is in the range[28] 5 to 10, the aforementioned dimensions and the test procedures recommended by RILEM (1985) were used to measure the fracture energy. The appetance of specimen dimensions and test procedures for evaluating the fracture energy of SFRC will be discussed.

The curing procedure was consisted on the following steps: first week in a wet chamber; immersed in water until 28 days; kept in a wet chamber until one week before testing. During this last week the specimens were prepared for testing. At midspan, in the opposite casting surface, a saw cut of 5 mm wide and 25 mm deepness was done with an appropriate equipment (see Figure 1). The tests were carried out with specimens of 400 to 500 days of age.

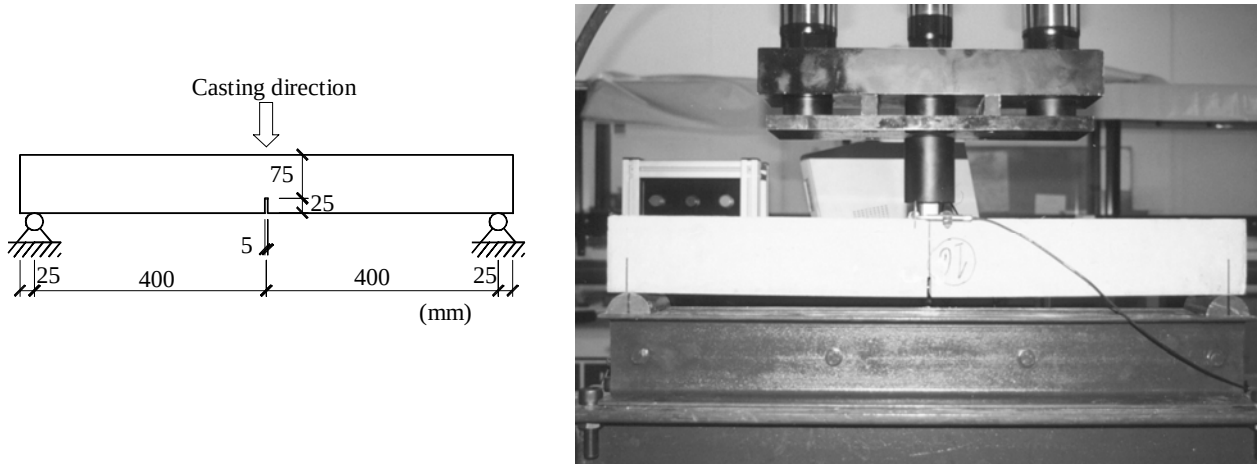

Figure 1 – Notched beam for three point bending tests.

3 – EQUIPMENT AND TEST PROCEDURES

During 1998 it was developed a servo-controlled equipment for static and dynamic tests on specimens and structural elements[23]. The equipment, the definition of the test procedures and their accomplishment are controlled by software. The hydraulic power station of the equipment was prepared for a maximum loading of approximately 400 kN. In the present state, the equipment has two triple actuators of 250 kN maximum load capacity, and can read eight channels of displacement transducers and four channels of force transducers or strain gages (gauges ?). Any of these transducers can be selected for testing control purposes.

Three cylinders compose a triple actuator. The cylinders at the actuator extremities have 100 kN maximum load capacity and the cylinder at the actuator centre has 50 kN maximum load capacity (see Figure 2). This actuator can work for loading limits of 250 kN, 200 kN and 50 kN, using the three cylinders, the lateral cylinders only, or the central cylinder only, respectively. In this way, the loading level can be selected, taking into account the predicted maximum load in the test, enhancing the test stability and the test control performance. In the

conception of the triple actuator it was also taken into account the aim of carrying out stable tests with specimens of low bearing capacity, which is the case of the notched beam specimens for evaluating the fracture energy. Displacing the lateral actuators a pre-load is applied on the central cylinder (see Figure 2a). In the same way, displacing the central cylinder, a pre-load is applied on lateral cylinders (see Figure 2b). Therefore, a null force could never be registered in the active cylinders, which contributes for the test stability. The pre-loading level can be selected on the software developed.

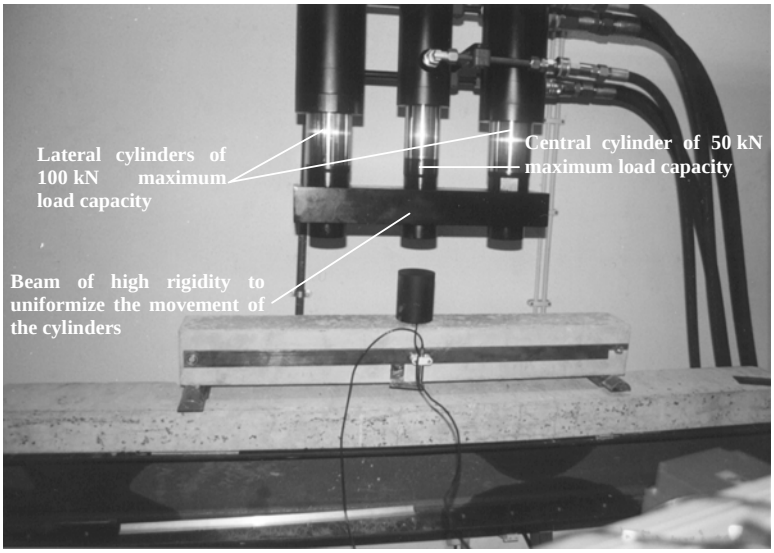

Figure 2 – Photo of the triple actuator.

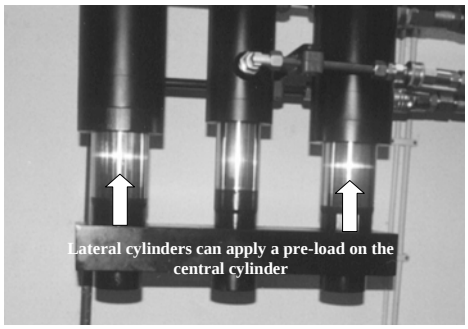

(a)

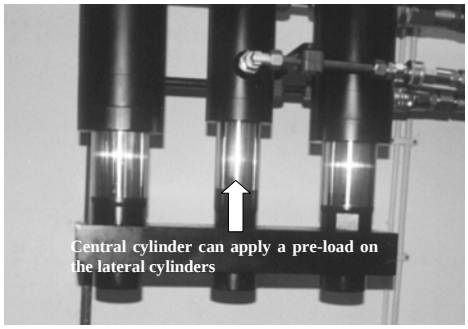

(b)

Figure 3 – Pre-loads that can be applied to the active cylinders.

To obtain the complete load-deflection relationship, the tests were carried out using displacement control. In order to avoid extraneous deformations, the middle point deflection was measured by a displacement transducer placed on a frame attached to the beam, the so-called "Japanese yok"[8,10], see Figure 4. The displacement transducer has a linear branch of 25 mm with 0.1% accuracy of the full scale.

The load was registered by a tension-compression force transducer of 20 kN maximum load capacity of 0.5% accuracy. Load was applied through fixtures that allowed for rotational freedom. The load was distributed in the beam width using a steel bar of 95×20×20 mm^3 dimensions.

Figure 5 shows the structure supporting the test set-up. It consists of HEB 200 steel profiles, setting up a frame that offers reaction to the actuator. The final configuration of the reaction frame was established after some preliminary tests that revealed the need of using very stiff reaction frames for assuring the stability of this type of tests.

The loop gain of the data acquisition cartridge was also another parameter calibrated during the preliminary tests, since it was observed that the system behaviour was very sensitive to this parameter. The loop gain should be increased when the ratio between the specimen stiffness and the supporting structure stiffness is increased.

The tests were carried out using the following deflection rates: 2.5 μm/s until 100 μm of deflection, 5 μm/s between 100 and 200 μm of deflection; 10 μm/s between 200 and 2300 μm deflection. Among the three load regimes available on the triple actuator, it was selected the lowest, 50 kN, using the central cylinder. In order to enhance the test stability, a pre-load of 16 kN was applied to the central cylinder. The force and the displacement were registered every second. The data was saved on a file for posterior post-processing.

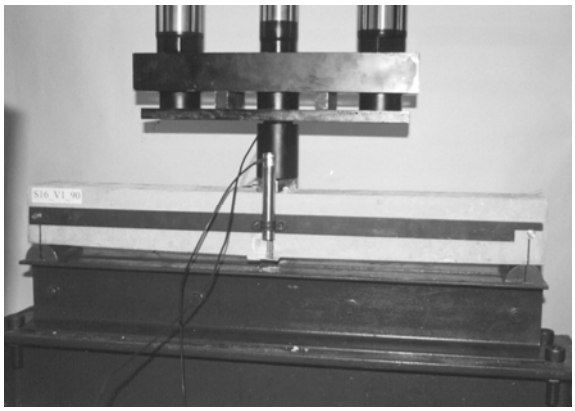

Figure 4 – Device for displacement measuring.

Figure 5 – Equipment and reaction frame.

4 – RESULTS

The force-deflection relationship registered on specimens reinforced with 30, 60 and 90 kg/m^3 of fibres was shown in Figures 6 to 8. The "average" force-deflection relationship for each series is depicted in Figure 9. The "average" force-deflection relationship for a given series was obtained determining, for each deflection, the average force of the tests of this series.

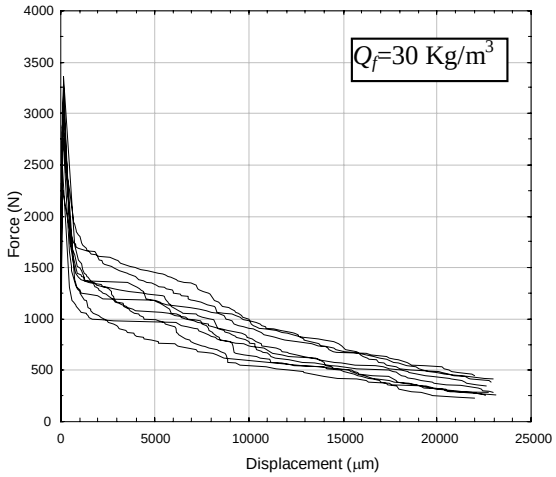

Figure 6 – Force-deflection relationship for series of 30 kg/m^3 of fibres.

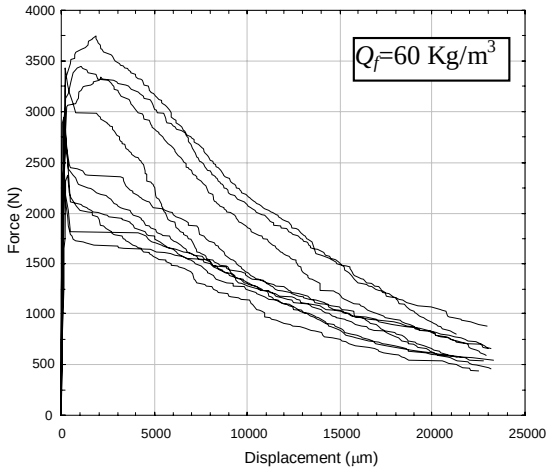

Figure 7 – Force-deflection relationship for series of 60 kg/m^3 of fibres.

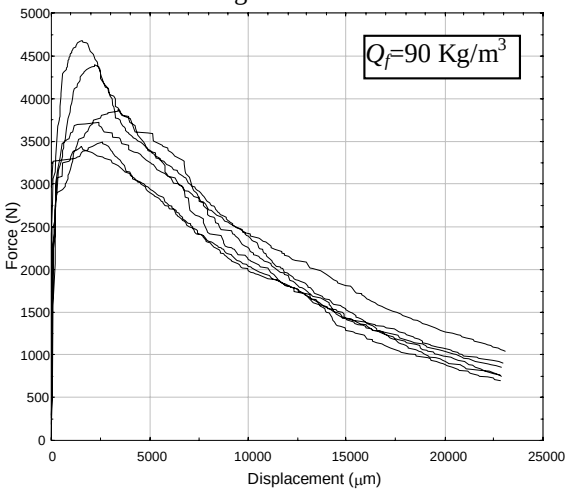

Figure 8 – Force-deflection relationship for series of 90 kg/m^3 of fibres.

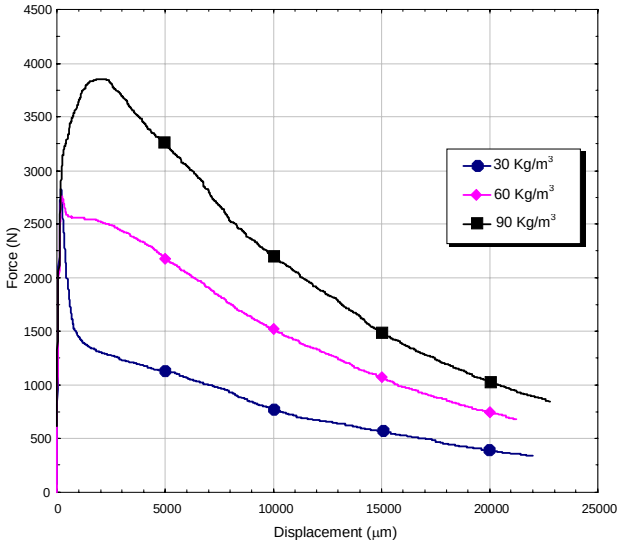

Figure 9 – "Average" force-displacement relationship for series of 30, 60 e 90 kg/m^3 of fibres.

The maximum force and the maximum stress at notched cross section for the three contents of fibres are represented in Figures 10 and 11. The maximum stress at notched cross section was evaluated from the following expression

$$\sigma_{max} = \frac{3}{2}\frac{F\ell}{b(h-a)^2} \tag{1}$$

where F is the maximum load, ℓ is the specimen span (= 800 mm), b and h are the width and the height of the specimen (=100 mm) and a is the depth of the notch (=25 mm).

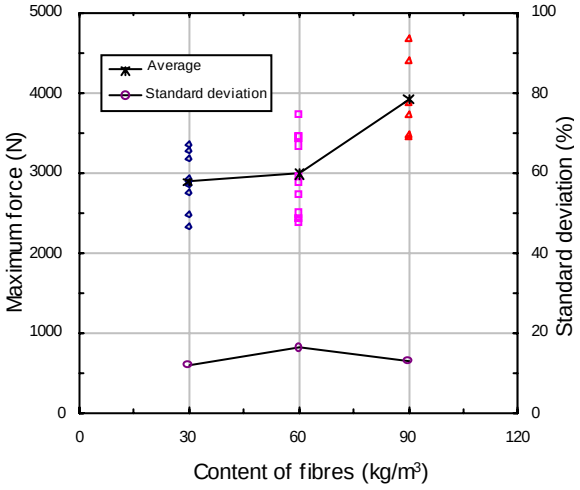

Figure 10 – Maximum force.

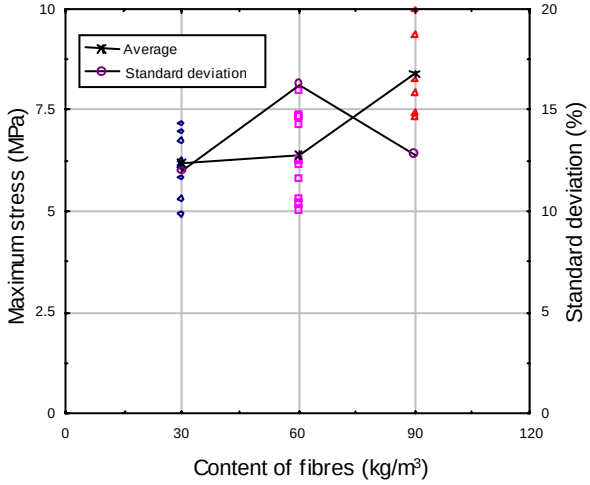

Figure 11 – Maximum stress at notched cross section.

(??? Legendas a letra maior. Para a revista tudo a preto. A cores para a apresentação ???)

From the results obtained it can be pointed out the following notes:

- A significant dispersion of the results was observed, mainly in specimens reinforced with 60 kg/m^3 of fibres, which reveals that it is necessary to improve the procedures of mixing the fibrous compositions in order to assure a homogeneous distribution of fibres into concrete;
- The maximum load in series reinforced with 30 and 60 kg/m^3 of fibres is almost the same;
- The maximum load increases significantly in specimens reinforced with 90 kg/m^3 of fibres;
- The decline of the force after peak load decreases with the increment of fibre content;
- In specimens reinforced with 90 kg/m^3 of fibres a hardening branch was developed after the first crack deflection, due to the high percentage of fibres bridging the crack surfaces;

For a very ductile specimens, such as the ones tested in the present work, it is important to account for the following two aspects:

a) The two “fixed” points of the bar, to which is attached the controller displacement transducer (see Figure 4) does not remain fixed for large deflections, as it is schematically represented in Figure 12. If specimens are supported in rollers, such is the usual practice,

these two points go upward with the deflection increment, adding a supplementary displacement registered in the controller displacement transducer. This supplementary displacement must be measured from two displacement transducers, located at these "fixed" points and their average value must be deducted from the displacement registered in the controller transducer. Otherwise, the energy absorption capacity evaluated will be larger than the real one.

b) For large deflections the compression strain in concrete volume, near the line load might (?) be greater than the linear elastic strain limit of SFRC. For ductile fibrous concrete, the energy dissipated in nonlinear behaviour of concrete in compression could be significant, mainly, when the notched deepness is less than half height of the specimen. This energy should be evaluated and deducted from the energy determined using the registered force-displacement relationship. The energy dissipated in compression can be evaluated from experimental or numerical strategies. Adopting experimental strategie, displacement transducers or strain gauges should be placed in the third half of the specimen height and the volume of concrete in compression nonlinear behaviour should be measured. In the numerical strategie, the energy dissipated in compression can be evaluated using a model that accounts for the material constitutive laws.

In the present work the displacement of the "fixed" points of the bar was evaluated assuming the specimen as a two rigid blocks rotating in turn of the point P (see Figure 12). This displacement was deducted from the deflection registered in the control displacement transducer. For specimens dimensions used in the present work the displacement of the "fixed" points was 0.164 mm for a deflection of 20 mm, i.e., 0.8%. However, for specimens with dimensions of 450×150×150 mm, adopted for evaluating the toughness indices[8,10], an error of 4.5% is done for 20 mm of ultimate deflection, which should not be despisted[9].

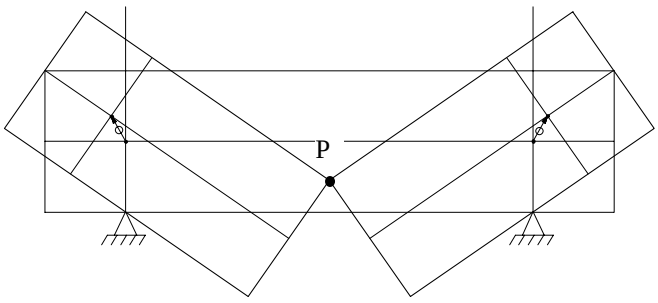

Figure 12 – The "fixed" points of the bar supporting the controller displacement transducer do not remain fixed for large deformations.

Table 4 includes the error on the energy when the displacement of the "fixed" points of the "Japanese yok" bar was not taken into account. It can be concluded that, for the specimen dimensions and notch deepness adopted the error is reduced. The error will be even lesser because the approach used for evaluating the displacements of the "fixed" points gives upper bond values.

Table 3 – Energy until ultimate deflection

Content of fibres (Kg/m^3)	U_L (1) (N.mm)	U_R (2) (N.mm)	$\frac{\lvert U_L - U_R \rvert}{U_R} \times 100$ (%)
30			
60			
90			

(1) U_L - energy evaluated from the registered force-deflection relationship

(2) U_L - energy evaluated from the force-corrected deflection relationship

In figure 13 it is depicted the energy dissipated for the series tested. This energy was evaluated from the force-corrected deflection relationship until a corrected deflection of about 23 mm. It was observed that, for content of fibres between 30 to 90 kg/m^3, the increment on energy is almost linear. This tendency was already registered in previous work[14]. The dispersion of the results is also remarkable, mainly in series reinforced with 60 kg/m^3 of fibres. The main results obtained are included in Table 4. In plain concrete specimens with a composition equal to that of Table 2, it was obtained a maximum bending stress on notched cross section of de 4.6 MPa and an energy of 1690 N.mm. These specimens had dimensions of $450 \times 150 \times 150$ mm^3 and a notch deepness of half beam height.

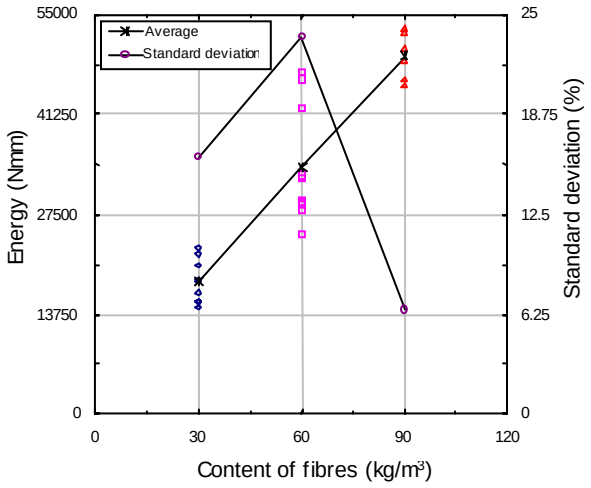

Figure 13 – Energy dissipated.

(??? Corrigir. Legendas a letra maior. Para a revista tudo a preto. A cores para a apresentação ???)

Table 5 – Most significant results.

Content of fibres (kg/m^3)	Maximum force (N)	Maximum stress (MPa)	Energy (N/mm) ***
30	2894	6.2	??
60	2983	6.4	??
90	3935	8.4	??

*** until deflection of 23 mm

6 – EVALUATING THE FRACTURE ENERGY

In order to evaluate the energy dissipated in compression, a cross sectional layer mode was applied. Figure 14 represents schematically this model. A full description of this model can be found elsewhere[14].

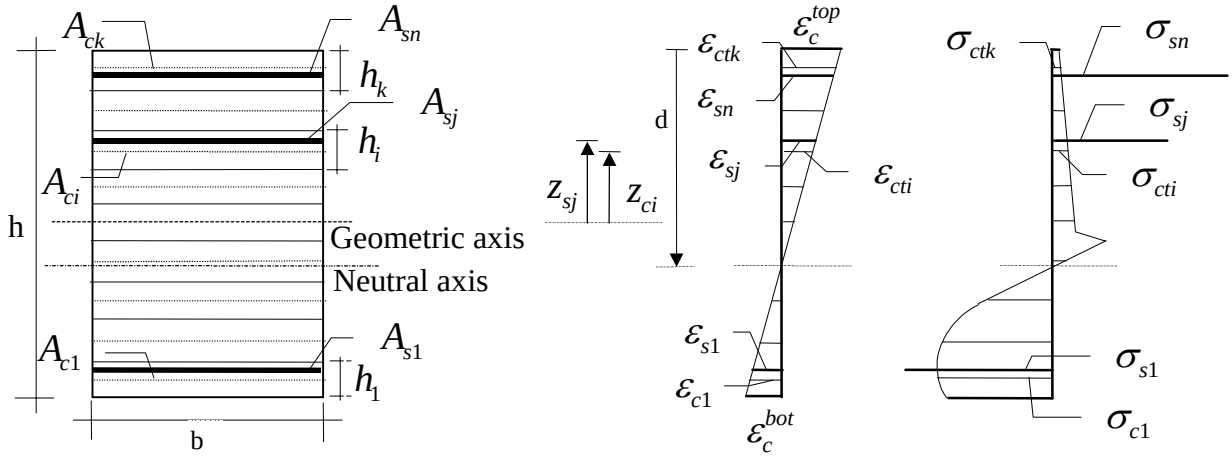

(a) Cross section (b) Strain distribution (c) Stress distribution

Figure 14- Cross section discretization and assumed strain and stress diagrams.

To evaluate the energy dissipated in compression it is necessary to determine the volume of the concrete where the compression strain overpass the linear elastic compression strain. This volume was designated by damaged zone, because encompasses the concrete nonlinear behaviour in tension as well as in compression (Figure 15). This damaged region should have a shape like the one represented in Figure 16. In the present approach it was assumed that the damaged zone grows up from notch mouth until beam top surface taking a sloping of 45 degrees. The beam was assumed as two linear elastic regions (intact concrete) connected by a damaged region, ahead of the notch (Figure 16). The width of the damage zone was determined using the cross sectional layer model, fitting the experimental force-deflection data (Figure 17).

Figure 15 – Schematic representation of specimen for model use.

Figure 16 – Damaged zone discretized in concrete layers.

Figure 17 – Comparision between the results obtained with the cross sectional layer model and experimental data.

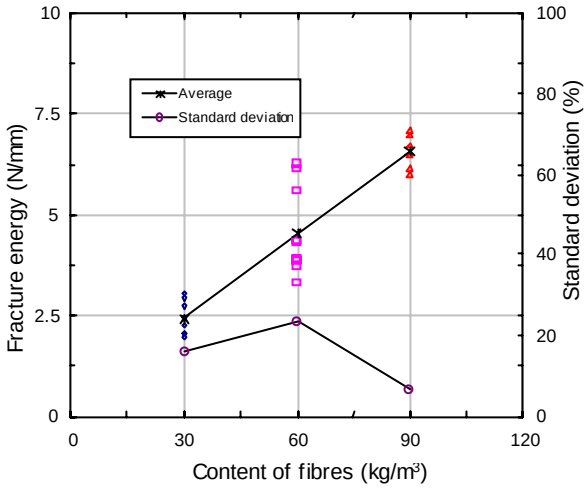

Figure 13 – Fracture energy.

6 – EQUIVALENT FLEXURAL STRENGTH

7 – CONCLUSIONS

In this work it is described the three point bending notched beam tests under dispacement control for evaluating the energy absorption capacity of concrete reinforced with 30, 60 and 90 Kg/m^3 of hooked-ends steel fibres.

From the results obtained, a significant increase on the maximum force was only observed on specimens reinforced with 90 Kg/m^3 of fibres. The energy absorption capacity was increased almost linearly with the fibre content, which assures previous results. A scatter on the results was observed which reveals difficulties on guarantee a homogeneous fibre distribution in concrete. Due to the fact that the first-crack deflection is difficult to determine reliably, a

large scatter was registered on this deflection, was well as, on the peak load deflection. The major part of the toughness indices are based on multiples of the first-crack deflection, and consequently, a large scatter is usually observed on the toughness indices, which reduces their applicability on designing practice.

8 – BIBLIOGRAFIA

[1] - P.N. Balaguru, S.P. Shah, *Fiber reinforced cement composites*, McGraw-Hill International Editions, Civil Engineering Series, (1992).

[2] - A. Nanni and A. Johari, "RCC pavement reinforced with steel fibers", *Concrete International*, 64-69, April, (1989).

[3] - P.C. Tatnall and L. Kuitenbrouwer, "Steel fiber reinforced concrete in industrial floors", *Concrete International*, 43-47, December, (1992).

[4] - , M. Vandewalle, *Tunnelling the world*, N. V. Bekaert S.A., (1990).

[5] - J.A.O. Barros, J.A. Figueiras "Experimental behaviour of fiber concrete slabs on soil", *Journal Mechanics of Cohesive-frictional Materials*, Vol. 3, 277-290, (1998).

[6] - J.A.O. Barros, "Experimental behavior of mesh reinforced shotcrete and steel fiber reinforced shotcrete panels", *International Conference of the European Ready Mixed Concrete Organization, ERMCO'98*, Lisboa, 23-27 Junho, (1998).

[7] – V.S. Gopalaratnam, S.P. Shah, G.B. Batson, M.E. Criswell, V. Ramakrishnan, M. Wecharatana, "Fracture toughness of fiber reinforced concrete", *ACI Materials Journal*, 88(4), 339-353, July-August, (1991).

[8] - J.A.O. Barros, *Comportamento do betão reforçado com fibras - análise experimental e simulação numérica* Tese de Doutoramento, Faculdade de Eng. da Univ. do Porto, (1995).

[9] – J.A.O. Barros, "Caracterização do comportamento do betão reforçado com fibras de aço por intermédio de ensaios experimentais", *1as Jornadas de Estruturas de Betão, Betões de Elevado Desempenho, Novos Compósitos*, 151-170, Outubro, (1996).

[10] - ??

[11] – JSCE - The Japan Society of Civil Engineers, *Part III - 2 method of tests for steel fiber reinforced concrete*, Concrete Library of JSCE, Nº 3, (1984).

[12] - Hillerborg, A.,"Analysis of fracture by means of the fictitious crack model, particularly for fibre reinforced concrete", *The International Journal of Cement Composites*, Vol. 2, Nº 4, pp. 177-184, (1980).

[13] - De Borst, R., *Non-linear analysis of frictional materials*, Dissertation, Delft Univ. of Technology, (1986).

[14] - Rots, J.G., *Computational modeling of concrete fracture*, Dissertation, Delft University of Technology, (1988).

[15] - J.A.O. Barros, "Analysis of concrete slabs supported on soil", *IV Congreso de Métodos Numéricos en Ingeniería*, Sevilha, Junho, (1999) (invited paper).

[16] - Barros, J.A.O., Figueiras, J.A., "Flexural behavior of steel fiber reinforced concrete: testing and modelling", *Journal of Materials in Civil Engineering, ASCE*. (accepted for publication).

[17] – Dramix *Steel fibre reinforced industrial floor design in accordance with the Concrete Society TR34*, N.V. Bekaert S.A., Responsible editor: H. Thooft - Zingem (1997).

[18] - RILEM TC 50-FMC, "Determination of fracture energy of mortar and concrete by means of three-point bend tests on notched beams", *Materials and Structures*, 18(106), 285-290, (1985).

[19] – D.A. Hordijk, *Local approach to fatigue of concrete*, PhD Thesis, Delft University of Technology (1991).

[20] - Wang, Y. ; Li, V.C. ; Backer, S., "Experimental determination of tensile behaviour of fibre reinforced concrete", *ACI Materials Journal*, Vol. 87, Nº 5, pp. 461-468, September-October, (1990).

[21] – Gopalaratnam, V.S.; Gettu, R., "On the characterization of flexural toughness in FRC", Workshop on Fibre Reinforced Cement and Concrete, Sheffield, U.K., July 28-30, (1984).

[22] - F. Freitas, J.A.O. Barros, P. Fonseca, *Manual de utilizador do equipamento SENTUR - versão 1.0*, Departamento de Engª Civil da Escola de Engª da Universidade do Minho, (1998).

[23] - Bekaert Specification, *Dramix fibres hors fils d'acier pour reinforcement de betón et mortier*, Bekaert N.V., (1991).

[24] – ACI 544 1996

[25] - J.M. Sena Cruz, *Comportamento cíclico de estruturas porticadas de betão armado reforçadas com fibras de aço*, Tese de Mestrado, FEUP, (1998).

[26] – referir o ACI 544 1996

[27] - CEB-FIP Model Code 1990 (1993). *Comite Euro-International du Beton*, Bulletin d'Information nº 213/214, Ed. Thomas Telford.

[28] - Hillerborg, A., *Concrete fracture energy tests performed by 9 laboratories according to a draft RILEM recommendation*, Report to RILEM TC50-FMC, Report TVBM-3015, Lund Sweden, (1983).

[29] - Trottier, J.-F. and Banthia, N. (1994). "Toughness characterization of steel-fiber reinforced concrete." *J. Materials Civ. Engrg.*, ASCE, 6(2) 264-289.

[20] – P. Casanova, *Bétons renforcés de fibres métalliques – du matériau à la structure*, Tese de Doutoramento, LCPC, (1996).